Machine-Learning blends of geomorphic descriptors: value and limitations for flood hazard assessment across large floodplains

Andrea Magnini[1], Michele Lombardi[2], Simone Persiano[1], Antonio Tirri[3], Francesco Lo Conti[3], and Attilio Castellarin[1]

[1]Department of Civil, Chemical, Environmental and Materials Engineering (DICAM), University of Bologna, Bologna, Italy
[2]Department of Computer Science and Engineering (DISI), University of Bologna, Bologna, Italy
[3]Leithà, Unipol Group, Milan and Bologna, Italy

Correspondence: Andrea Magnini (andrea.magnini@unibo.it)

Abstract. Recent literature shows several examples of simplified approaches that perform flood hazard (FH) assessment and mapping across large geographical areas on the basis of fast-computing geomorphic descriptors. These approaches may consider a single index (univariate) or use a set of indices simultaneously (multivariate). What is the potential and accuracy of multivariate approaches relative to univariate ones? Can we effectively use these methods for extrapolation purposes, i.e. FH assessment outside the region used for setting up the model? Our study addresses these open problems by considering two separate issues: (1) mapping flood-prone areas, and (2) predicting the expected water depth for a given inundation scenario. We blend seven geomorphic descriptors through decision tree models trained on target FH maps, referring to a large study area ($\sim10^5$ km^2). We discuss the potential of multivariate approaches relative to the performance of a selected univariate model and on the basis of multiple extrapolation experiments, where models are tested outside their training region. Our results show that multivariate approaches may (a) significantly enhance flood-prone area delineation (accuracy: 92%) relative to univariate ones (accuracy: 84%), (b) provide accurate predictions of expected inundation depths (determination coefficient ~0.7), and (c) produce encouraging results in extrapolation.

1 Introduction

Every year flood events worldwide cause vast economic losses, as well as heavy social and environmental impacts, which have been steadily increasing over the last five decades (Jongman et al., 2014; Guha-Sapir et al., 2016), mainly because of the complex interaction between the intensification of extreme hydrological events due to climate change (e.g., Brunetti et al., 2002; Uboldi and Lussana, 2018) and anthropogenic pressure (i.e., land-use and land-cover modifications, see Di Baldassarre et al., 2013; Domeneghetti et al., 2015; Requena et al., 2017). Thus, nowadays, successful flood hazard mapping for flood hazard management is a major task for the whole scientific community (Alfieri et al., 2014; Dottori et al., 2016). Traditional methods to assess fluvial flood hazard rely on hydrological and hydraulic numerical models, whose improvement allows to simulate any scenario for different geometrical or hydrological conditions, obtaining very accurate results (Horritt and Bates, 2002; Costabile et al., 2012; Bellos and Tsakiris, 2016). However, a high amount of hydrologic and hydraulic input information is required to adequately describe the geometry and hydraulic behaviour of the system, thus considerable effort and computation

capacity are needed. Consequently, numerical models are unsuitable for large-scale applications and in data-scarce regions.

25 To overcome this issue, other mapping techniques have been proposed that take advantage of the wealth of topographic information contained in digital elevation models (DEMs): flood-related geomorphic descriptors (or features, or indices) can be derived from DEMs and used to obtain a measure of flood hazard.

The first DEM-based approaches proposed in the literature (see e.g., Williams et al., 2000; Noman et al., 2001; Dodov and Foufoula-Georgiou , 2006; Nardi et al., 2006; Manfreda et al., 2011, 2014, 2015; Samela et al., 2017; De Risi et al., 2018)

30 consider a single geomorphic index (these approaches will be referred to as univariate hereafter), which is used as a binary classifier to distinguish between flood-prone and flood-free areas through the definition of a threshold value. The optimal threshold value is identified by means of an iterative calibration procedure which optimizes the agreement of the binary map with a reference pre-existing flood hazard map obtained, e.g., from hydrological-hydraulic numerical simulations. Several authors (see e.g., Manfreda et al., 2015; Samela et al., 2017) highlight that the performance of the considered geomorphic index can

35 change according to the geographical context of the application. In particular, the descriptor named Geomorphic Flood Index (GFI; Samela et al., 2017) has been shown to have good effectiveness in mountainous as well as in predominantly flat areas, and thus has been used extensively by many authors for developing web-services, platforms, and GIS tools for flood-hazard mapping applications (Samela et al., 2018; Tavares da Costa et al., 2019). A second class of DEM-based approaches to be investigated can be named as multivariate, as they rely on the combination of different geomorphic descriptors (GDs). The

40 relation between the combination of GDs and flood hazard can be searched through numerous statistical methods. Commonly, Machine Learning (ML; Breiman, 1984) models are used, often ensembled with multi-criteria decision-making techniques (Triantaphyllou et al., 2000; Ho et al., 2010). Some authors (Degiorgis et al., 2012; Gnecco et al., 2017) have tested a blend of GDs, while some others mixed these indices with information on land use, soil geology and climate, and compared different combination strategies (e.g., Wang et al., 2015; Lee et al., 2017; Khosravi et al., 2018; Arabameri et al., 2019; Janizadeh et al.,

45 2019; Costache et al., 2020). These studies suggest that data-driven flood hazard mapping has a remarkable potential. However, in most of the studies, the reference flood hazard information used to set up the models consists of a dataset of isolated historical events observed in the study area (Lee et al., 2017; Khosravi et al., 2018; Janizadeh et al., 2019; Arabameri et al., 2019; Costache et al., 2020), leading to case-specific prediction skills.

Important advantages of DEM-based flood hazard mapping methods are their flexibility and, in principle, their general applica-

50 bility to any flood-prone area where a reliable DEM is available, as well as their low computational costs relative to numerical models. However, two main drawbacks must be highlighted: first, DEM-based methods do not consider the water dynamics, and second, they need a pre-existing reliable reference flood hazard map, which may or may not be available for the area of interest. Overall, DEM-based models are very useful as preliminary flood hazard mapping tools in data-scarce contexts and in application to large areas, but cannot yet effectively substitute the traditional models, especially when detailed results are

55 required. Nevertheless, if a strong and reliable relation to derive flood hazard from GDs is obtained, the model could be easily applied in extrapolation to any region where the same relation is supposed to be valid (Tavares da Costa et al., 2020).

In this study, multivariate DEM-based flood hazard mapping is investigated. We consider a large study area ($10^5 km^2$) in Northern Italy, which is characterized by markedly different morphological, hydrological and climatic conditions. We use the $\sim 90m$

resolution, hydrologically-corrected, MERIT DEM (Yamazaki et al., 2017) for deriving a set of GDs. We then use decision trees, a common machine learning technique (Hastie et al., 2009), for assessing flood hazard associated with a given probability of occurrence (i.e., return period) in terms of (a) delineation of flood-prone and flood-free areas, and (b) prediction of expected inundation water depth (as a measure for flood intensity). The simultaneous combination of the five following meaningful elements makes our study different from all previous works in literature. First, only strictly easy-to-retrieve, DEM-based GDs are used to assess flood hazard, in contrast with several studies in which also other information is considered. Second, both generation of binary flood susceptibility maps and prediction of expected maximum inundation water depth are analyzed, setting up parallel models. Third, decision trees are trained using pre-existing flood hazard maps as target information, in contrast with the discontinuous datasets of historical events mostly used to train machine learning models for flood hazard estimation (Lee et al., 2017; Khosravi et al., 2018; Janizadeh et al., 2019; Arabameri et al., 2019; Costache et al., 2020). Fourth, a univariate geomorphological approach for identification of flood-prone and flood-free areas (i.e., GFI) is compared with the proposed multivariate approach: this allows us to analyse the actual enhancement resulting from the use of multiple GDs. Fifth, predictive skill of the multivariate DEM-based flood hazard approach is assessed in extrapolation by applying models trained on specific geographical areas to different regions with dissimilar morphological and/or hydrological features. This last aspect is highly important for possible future applications to data-scarce environments in extrapolation mode.

By assuming the abovementioned characteristics, this study aims to advance previous knowledge on the potential of ML techniques for combining GDs to derive accurate flood susceptibility maps across large geographical regions. More precisely, we want to investigate three main research questions: (1) can we profit from a blend of various GDs for flood hazard assessment and mapping relative to a univariate approach? (2) Can we use simple ML techniques for effectively blending multiple GDs? (3) Are these techniques capable of providing a reliable assessment of flood hazard over large geographical areas when used in geographical extrapolation? What are the desired characteristics of the training region/watershed to make the trained model as general as possible?

The paper is organized as follows: Section 2 describes the methods (GDs and decision trees); Section 3 illustrates the study area and data; Section 4 details the analyses we performed; Section 5 shows the results and Section 6 discusses them.

2   Methods

The analyses conducted in the study are based on two main elements: geomorphic descriptors (GDs) and decision trees (DTs); simplicity and replicability of these elements represent a fundamental aspect and an important advantage of this contribute. Aiming to estimate flood hazard output variables (i.e., flood-susceptibility and maximum expected water depth), DTs models combine several selected DEM-derived input features (GDs), based on the availability of target information (i.e., flood hazard reference maps). Consistent with the aims of our study, we set up two different types of DTs: classifier DTs to solve the classification problem relative to flood-extent delineation, and regressor DTs to solve the regression problem of water depth estimation. Classifier and regressor models use the same input GDs, but require different target flood hazard maps. The software

we use for the training is Scikit-learn (Pedregosa et al., 2011), open source library for Python 3.6 or later (Van Rossum et al., 1995).

2.1 Geomorphic descriptors

Topographical rasterized information contained in DEMs can be used to extract GDs adopting several algorithms available in the literature (e.g., Tarboton et al., 1991). These descriptors vary spatially, assuming different values for different pixels within the domain, while being constant in time. They can be divided into two broad categories: (1) single features, if they represent simple terrain characteristics, and (2) composite indices, if they are derived based on a combination of other features. As input variables for the above-mentioned models, in our study we use the ground elevation in m a.s.l. itself (as retrieved from the DEM) together with six GDs, the first three of which are single indices, while the remaining three are composite:

1. **Local slope (sd8)**, estimated for each cell as the maximum slope among the eight possible flow directions and computed as the ratio between the vertical and the horizontal differences

2. **Horizontal distance from the nearest stream (D)**, defined as the length of the path that hydrologically connects each cell to the nearest cell of the river network

3. **Height above the nearest drainage (HAND)**, defined as the vertical difference between a given cell and the hydrologically nearest cell belonging to the river network (Rennò et al., 2008)

4. **Modified topographic index (TI_m)**, derived from the modification proposed by Manfreda et al. (2008) to the index originally introduced by Kirkby (1975), and defined as follows:

$$TI_m = \ln\left(\frac{a_d^n}{\tan(\beta)}\right) \tag{1}$$

where a_d is the drained area per unit contour length, $\tan(\beta)$ is the local gradient, n is an exponent <1

5. **Geomorphic flood index (GFI)**, defined as the ratio between the term h_r and HAND. The numerator represents the water depth, computed in the hydrologically nearest stream section with a hydraulic scale relation ($h_r \cong bA_r^n$, where A_r is the contributing area in the considered stream section). Coefficient b and exponent n can be appropriately estimated with calibration or taken from the literature (Nardi et al., 2006)

$$GFI = \ln\left(\frac{h_r}{HAND}\right) \tag{2}$$

6. Alternative version of the GFI, hereinafter referred to as **local geomorphic flood index (LGFI)**, defined as:

$$LGFI = \ln\left(\frac{h_l}{HAND}\right) \tag{3}$$

where the water depth h_l is computed with reference to the contributing area of the considered pixel

The choice of the above mentioned GDs is due to different reasons. First, previous studies (e.g., Manfreda et al., 2015; Samela et al., 2017) clearly showed that D and HAND are the most descriptive single-feature indices for flood hazard mapping, sufficiently accurate in mountainous regions, but still inadequate over predominantly flat areas, whereas, among composite feature indices, GFI and LGFI show good performance in both the geographical contexts. Also, in several studies (e.g., Wang et al., 2015; Lee et al., 2017; Khosravi et al., 2018; Janizadeh et al., 2019; Costache et al., 2020), elevation retrieved from DEM shows to have a strong influence on flood occurrence. Slope appears to be the most important index in Khosravi et al. (2018) and Costache et al. (2020), and among the most influent ones in Arabameri et al. (2019). The adoption of TI_m is based on Manfreda et al. (2008), who highligthed a strong correlation between the index and the occurrence of inundation events.

Indeed, we believe that the selected set of GDs provides DT models with a rather exhaustive description of the study area morphology. In fact, slope and TI_m may influence the infiltration time, and consequently the runoff; elevation is not only strongly linked to the runoff, but also to climatic conditions; D and HAND consider the horizontal and vertical proximity to the river network, and GFI and LGFI combine this information with an estimation of the water depth in the nearest stream. Overall, for the aim of a multivariate analysis, this combination should enable one to consider two comprehensive pieces of information by looking into the morphology (i.e. elevation, sd8, TI_m) and hydrology (i.e., by accounting for the river network; i.e. D, HAND, GFI, LGFI) of the study region.

2.2 Decision trees

Supervised ML models can be thought of as complex, parameterized functions that are trained to accomplish a specific task. In so-called supervised learning, training algorithms determine the structure and parameters of the model, by observing a series of examples, i.e. input-output pairs. Decision trees (DTs) are very popular supervised ML techniques (Breiman, 1984; Hastie et al., 2009), as they are very effective in solving many kinds of classification or regression problems based on an easily-interpretable logic.

DTs search for a relation between input and target output by means of a recursive splitting, which is done through a set of nodes organized in a tree structure. Being the input of a DT a vector of values for a fixed set of "attributes" (or "features"), each node corresponds to a test to be performed on a single attribute in the input vector. Depending on the outcome of the tests on the nodes, the data is forwarded to one of a set of "child" nodes (see Figure 1). Leaves are the last nodes; they are labeled with an output value, such as a class or a number, that represents the tree output for the given input vector.

Training a decision tree consists in determining its structure, the test on each node, and the labels on the leaves. Most training algorithms operate by recursively splitting the training set, measuring the quality of each partition with object functions that reflect the degree of uniformity of the output values (see Sect. 4.2). Repeatedly, tests leading to the best partition are chosen, and child nodes are created accordingly. When some termination criterion is reached, e.g. a set in the partition is perfectly uniform or a maximum depth has been reached, the last nodes become leaves and they are labeled either with the most frequent class value (discrete case) or with the average of the output values (numeric case).

Predictions: for each leaf, the output variable equals the mode or mean of the target values in that leaf during training

Leaf:
n_3 samples

Leaf:
$n_4 = n_1 - n_3$ samples

Leaf:
n_5 samples

Leaf:
$n_6 = n_2 - n_5$ samples

Splitting rule 1 (e.g., $m_j < x$)

Splitting rule 2 (e.g., $m_k > y$)

Node 1:
n_1 samples with
M features

Node 2:
$n_2 = N - n_1$ samples
with M features

Splitting rule 0 (e.g., $m_i > 0$)

Roots:
Entire dataset: N samples with M input features

Figure 1. Example structure of a decision tree for a given dataset with N samples and M features, having seven nodes in total: one root node, two decision nodes, and four leaves, resulting in an overall depth of three (i.e., longest path from roots to leaves)
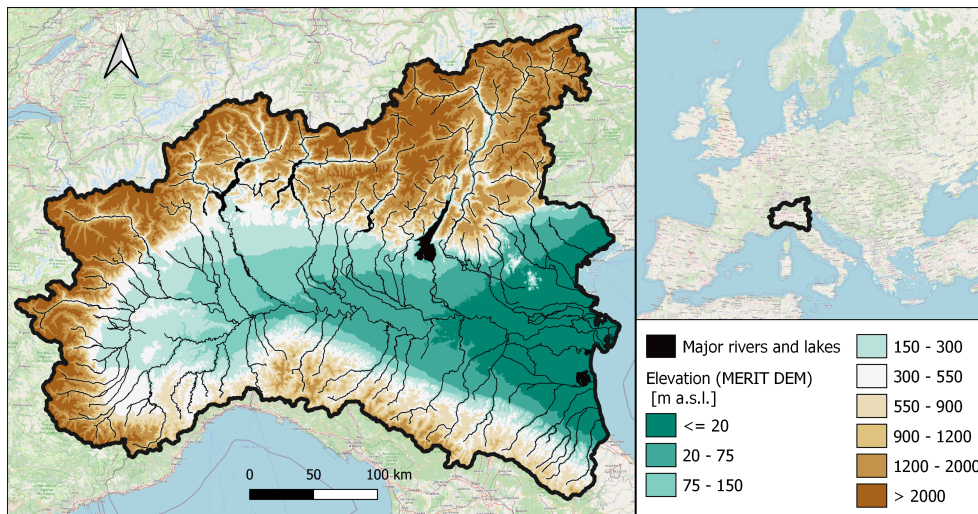
Figure 2. MERIT DEM for the study area, with major rivers and lakes marked in black (left); study area in the European context (right; map from ©OpenStreetMap contributors (2017), distributed under the Open Data Commons Open Database License (ODbL) v1.0)

3 Study area and data

The study area includes most of Northern Italy, and a little part of Switzerland, having a total extent of about $10^5 km^2$. Many different geographical subsystems can be found within this surface: the Alps, located in the North, lie in about $5 \cdot 10^4 km^2$, with average elevation of 2500 m a.s.l. and a mainly rocky soil. This mountain range also hosts several big lakes, as Garda,

Maggiore and Iseo Lakes. The Apennines, in the southern portion, have lower altitudes than the Alps, and more permeable
soils. The Po Valley, the largest floodplain in Italy, stretches from West to East, covering an area of about $4.6 \cdot 10^4 km^2$, going
from the Alps and the Apennines to the Adriatic Sea (see Figure 2). The study area is mostly occupied by the Po river basin,
that is the largest in Italy. Moreover, other important rivers are the Adige, Brenta, Reno and Bacchiglione. For this large and
predominantly flat region, floods represent a major issue, also considering its high population density and presence of strategic
industrial and agricultural assets (ISPRA, 2018; Persiano et al., 2020).

The DEM used to represent the study area is the freely-available Multi-Error-Remover Improved-Terrain model (MERIT;
see Yamazaki et al., 2017). This choice was made for two reasons. First, MERIT should be quite reliable for hydrological
applications, as it is the product of several processing operations and corrections on previously available DEMs (i.e., NASA
SRTM3 and JAXA AW3D), some of which specifically addressing hydrological consistency (e.g. agreement between modelled
and real stream-network). The second reason is that its resolution is 3 arcseconds, which corresponds to $\sim 90m$ at the equator.
These characteristics enabled us to perform an accurate computation of geomorphic indices, while reducing the computational
costs.

Two different freely-available reference flood hazard maps have been used to train the ML models. The first, used for the
classification problem (i.e., delineation of flood-extent), has been produced by the Italian Institute for Environmental Protection
and Research (ISPRA) to fulfill the Floods Directive of the European Parliament (2007/60/EC). This map (hereinafter referred
to as PGRA P1) refers to a return period of about 500 years and comes from the merge of different hazard maps produced
by local authorities, which explains its heterogeneity. Detailed flood hazard mapping characterizes some areas (e.g., see the
northwestern portion of the study area in Figure 3), while lacking information affects other zones (e.g., see the northeastern
portion of the study area in Figure 3). In the reminder of this study we term exhaustiveness the degree of detail by which
flood hazard is defined and captured for minor streams. The second map (see Figure 4), used for the regression problem (i.e.,
estimation of water depth), is made available by the study from the Joint Research Centre (JRC) of the European Commission
and refers to a return period of 100 years; it will be named JRC 100 in the remainder of the study. Differently from PGRA
P1, JRC 100 provides information in terms of water depth and is uniform throughout the study area, yet evenly incomplete
and less accurate for minor streams, as it comes from the merger of several numerical simulations, which considered only river
catchments with drainage area higher than $500 km^2$ (see Dottori et al., 2016).

4   Framework of the analysis

This section provides an overview of the four macro-phases of the present study, namely:

1. **Data selection and preparation**

    (a) Selection of the DEM and computation of geomorphic indices with terrain analysis

    (b) Selection of the flood hazard target map

2. **Preliminary analyses**
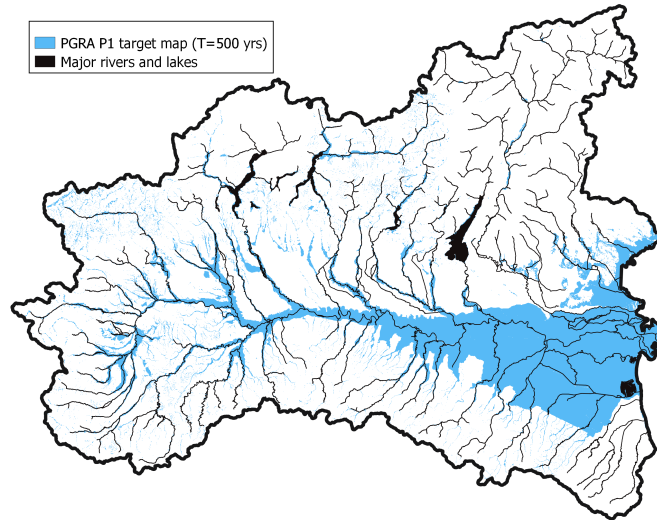
Figure 3. Binary flood hazard target map with return period ∼500 years, made available by ISPRA and termed PGRA P1 in this study
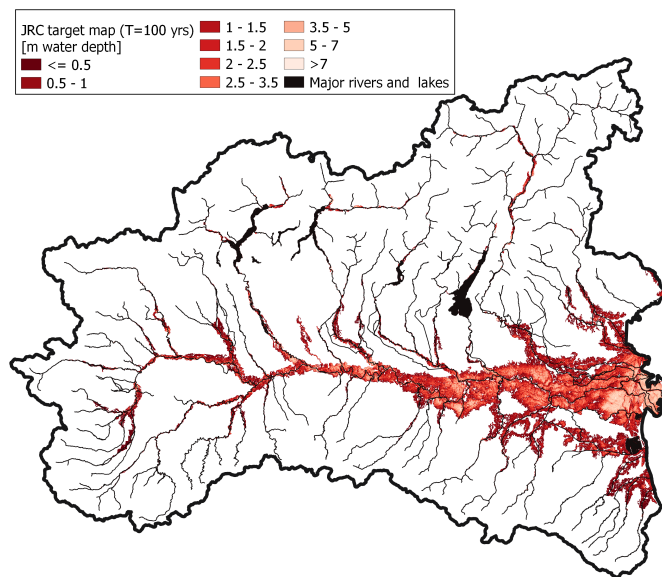
Figure 4. Water depth for the target 100-year flood hazard map obtained by Dottori et al. (2016), termed JRC 100 in this study (colour classes in the legend are used for data visualization only)

(a) Definition and preparation of the calibration area

(b) Selection of performance metrics and objective functions

3. **Implementation of the univariate approach (benchmark approach)**: set-up of GFI optimal threshold in randomly-selected 85% of calibration area

4. **Testing multivariate approach with two different modes:**

Testing mode	Training set	Testing set
Geographical interpolation	Randomly selected 85% of calibration area	Randomly selected 15% of calibration area
Geographical extrapolation	Geographical sub-region of the calibration area	Geographical remainder of the calibration area

190

Macro-phase (1) of the study consists of the preparation of input data, which is a fundamental step for the success of machine learning algorithms; specific criteria are used to select the GDs (Sect. 2.1), the accuracy and horizontal resolution of the DEM, and the target flood-hazard datasets (Sect. 3). Phase (2) (i.e., preliminary analyses) is necessary for defining some important aspects for the succesful set-up of DEM-based models: the calibration area (Sect. 4.1), the objective functions and the performance metrics for evaluating the results (Sect. 4.2). Phase (3) identifies the benchmarking approach, i.e. a univariate DEM-based model for classification of flood susceptible areas, to be used as comparison for the successive analysis. This model is built up according to the indications reported in the literature, and considers the GFI descriptor alone, as it is found to be the most versatile and accurate by many authors (e.g., Samela et al., 2017).

The main results of the study are obtained in phase (4), as the DEM-based multivariate approach is tested in two different ways. First, two DTs are set-up (i.e., one classifier DT and one regressor DT) using training and test sets with the same statistical distribution of input features. This represents an ideal case (termed here as *geographical interpolation mode*), in which the training and test sets have very similar morphoclimatic characteristics. Second, four sub-portions of the study area are selected based on specific morphoclimatic conditions, and then, eight more DTs are trained on these areas (i.e., one classifier DT and one regressor DT for each training area) and tested on the complement to the study region (see Sect. 4.3). This represents a data-scarce case (termed here as *geographical extrapolation mode*), in which morphoclimatic characteristics of training and test sets may be rather different.

4.1 Calibration area

Previous studies (e.g., Tavares da Costa et al., 2019) have highlighted that the DEM-based classification of regions into flood-prone and flood-free zones is more effective if the calibration is done on meaningful areas. This is due to the different importance of far-from-river and close-to-river pixels in the computation of the objective function. In the present study, training and testing of the models have been performed referring to a portion of the entire study area, which we term *calibration area*. Different methods to define this area have been tested during the preliminay analyses of phase (2), finding that the most effective way, representing a good trade-off between the calibration efficiency and the ease of identification, is to refer to a constant-radius buffer around the target flood hazard map. In particular, based on sensitivity analyses that clearly showed that the radius value has a non-negligible impact on the accuracy of the trained model, a 2 km radius has been selected for the PGRA P1 target map, and a 5 km radius for the JRC 100 map (see Figure 5). During our analyses, all the pixels falling outside
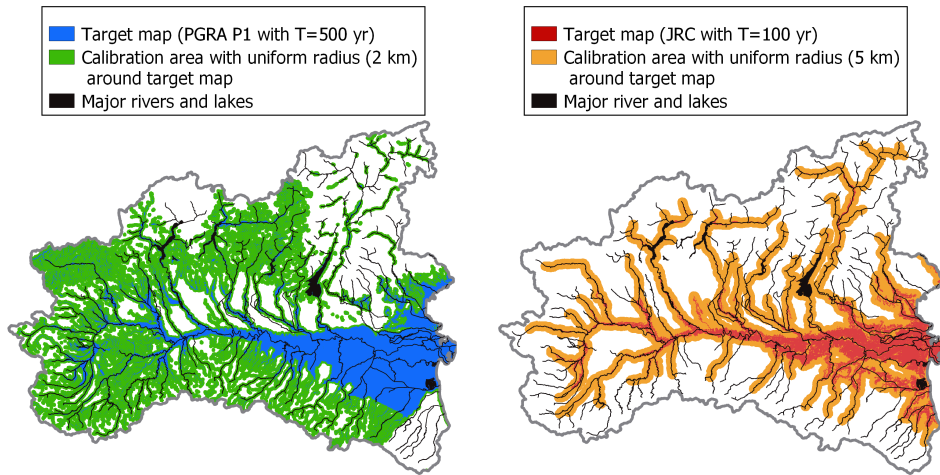
Figure 5. Calibration areas: 2km buffer (green) and PGRA P1 flood-prone areas (blue) used for the classification problem (left); 5km buffer (orange) and JRC 100 flood-prone areas (red) used for the regression problem (right)

the 2 km and 5 km calibration buffer areas are neglected when fitting the models and evaluating the results for all classification and regression problems, respectively.

4.2 Objective functions and performance metrics

220 Specific objective functions are used to train the DTs for classification and regression, while other performance metrics are computed to evaluate their predictions during the validation. With regards to the classification problem, the objective function, used during the training of the DTs to assess the quality of each split, is the Gini impurity ($I_G(p)$), that varies between 0 (the optimal value) and 1 (Hastie et al., 2009). At each step, the Gini impurity measures how often a randomly chosen element from the set would be incorrectly labeled if it was randomly labeled according to the distribution in the subset. Given the number of

225 target classes J, and the fraction of items labeled with class i in the set p_i, the Gini impurity is defined as follows:

$$I_G(p) = \sum_{i=1}^{J} p_i \cdot (1 - p_i) \tag{4}$$

To perform implementation of the univariate approach and parameterize the multivariate classifier DTs, and evaluate the results, we use the true skill statistic (TSS; Youden, 1950; Everitt et al., 2002), which is based on the contingency matrix, and varies between 0 and 1 (optimal value):

$$230 \quad TSS = \frac{TP}{TP + FN} + \frac{TN}{TN + FP} - 1 \tag{5}$$

where TP, TN, FP, FN are respectively true positive, true negative, false positive and false negative predictions of the model. TSS has been successfully used by several authors in different applications (Bartholmes et al., 2009; Alfieri et al., 2012; Tavares

da Costa et al., 2019). During preliminary analyses of phase (2), some experiments suggested to prefer this metric to accuracy (ACC, see below), which showed to be less sensitive to model modifications (i.e., different calibration areas, input information, tree depth) and goodness (lower extension of FP and FN areas).

Other metrics used for analysing the results are accuracy (ACC), precision (or positive predictive value, PPV), and recall (or true positive ratio, TPR). All the three are very common in evaluating the performance of a classifier (e.g., Manfreda et al., 2015; Samela et al., 2017). They all vary between 0 and 1 (optimal value), and are defined as follows:

$$ACC = \frac{TP+TN}{TP+TN+FP+FN} \tag{6}$$

$$PPV = \frac{TP}{TP+FP} \tag{7}$$

$$TPR = \frac{TP}{TP+FN} \tag{8}$$

With regards to the regression problem, the objective function to minimize during the training is the well-established mean squared error (MSE). Using n, $\hat{y}_i$ and and y_i to indicate respectively the number of samples, the predicted and the target value, MSE can be written as:

$$MSE = \frac{1}{n}\sum_{i=1}^{n}(y_i - \hat{y}_i)^2 \tag{9}$$

The metric mainly used to evaluate the results and parameterize the multivariate regressor DTs is the determination coefficient R^2, that varies between $-\infty$ and 1 (the optimal value). It measures the improvement of the predicted values relative to the mean of the input samples ($\overline{y}$), defined as:

$$R^2 = 1 - \frac{\sum_{i=1}^{n}(y_i - \hat{y}_i)^2}{\sum_{i=1}^{n}(y_i - \overline{y})^2} \tag{10}$$

The last considered metric is the mean absolute error (MAE), defined as:

$$MAE = \frac{1}{n}\sum_{i=1}^{n}|y_i - \hat{y}_i| \tag{11}$$

Lastly, we use the Gini importance (GI) to measure the importance of each factor (i.e., each GD) in the trained models (both classifier and regressor DTs), which is defined for the *j-th* factor as the total decrease in node impurity (I_{G_i}), weighted by the fraction of samples reaching that node (n_i). Although this measure is largely used for its speed of computation, it has the drawback of neglecting the weakest factor when two related factors are used, which has to be taken into account when discussing the results.

$$GI_j = \sum_{i=1}^{N_j}\frac{(I_{G_i} - I_{G_{i-1}})}{n_i} \tag{12}$$

where N_j is the number of nodes where a condition on the *j-th* factor is used as splitting rule.

4.3 Training and testing strategy

All models considered in this study are trained and tested in different sub-domains of their calibration area based on two different strategies. For the univariate model and the interpolation DTs, the pixels of the calibration area have been randomly split in 85% for the training and 15% for the test set, based on established proportion adopted for machine learning algorithms (Mosavi et al., 2018). This produces two datasets with millions of pixels, both with very diverse ranges of input and target information. During the extrapolation analyses, training is performed in turn on four different portions of the overall calibration area. To avoid dividing any catchment into a part for training and one for testing, the delineation of these areas follows catchment boundaries, as well as precise geographical and hydrological criteria (see Figure 6):

- **Area A** includes the Alpine catchments and the northern portion of the Po river floodplain. The complementary test area includes all the Apennines, a lower mountain range, and the southern part of Po plain, where smaller river catchments are located

- **Area B** includes catchments in the upstream sector of the Po river basin, representing part of the Alps and of the Apennines. The complementary test area includes most of the Po plain, and part of the Alps and Apennines

- **Area C** is the complementary of area B and consists of the downstream portion of the Po river basin

- **Area D** includes the Apennines, Western and Central Alps and the entire Po streamline. Its complementary test area contains a rather small part of the Po plain, the Western Alps and the flood plain of the Adige, Brenta and Bacchiglione rivers

Before training DTs, k-fold cross-validation (CV) is performed to optimize models hyper-parameters, namely: the maximum tree depth and the minimum number of records in any leaf node. K-fold CV is a widely used method for model parameterization and selection (Hastie et al., 2009), and consists in dividing the training set into k folds and then performing two consecutive operations: (1) training of the model using $k-1$ folds, and (2) validation of the model using the remaining fold. These two steps are repeated for k times, for all the combinations of the k folds of the training data.

5 Results

The reliability of the predictions of the models is assessed by performance metrics that refer to (a) the training set and (b) the test set. While the metrics computed for the training set assess the reliability in reproducing the observed target map, the ones regarding the test set measure the ability of the model when applied to a different sample than the one used in training (i.e. validation of the model). In order to find out the relevance of each input GD in the DTs' structure, the Gini importance (see Sect. 4.2) for each model is reported in Table 3, and will be better discussed in Sect. 6.
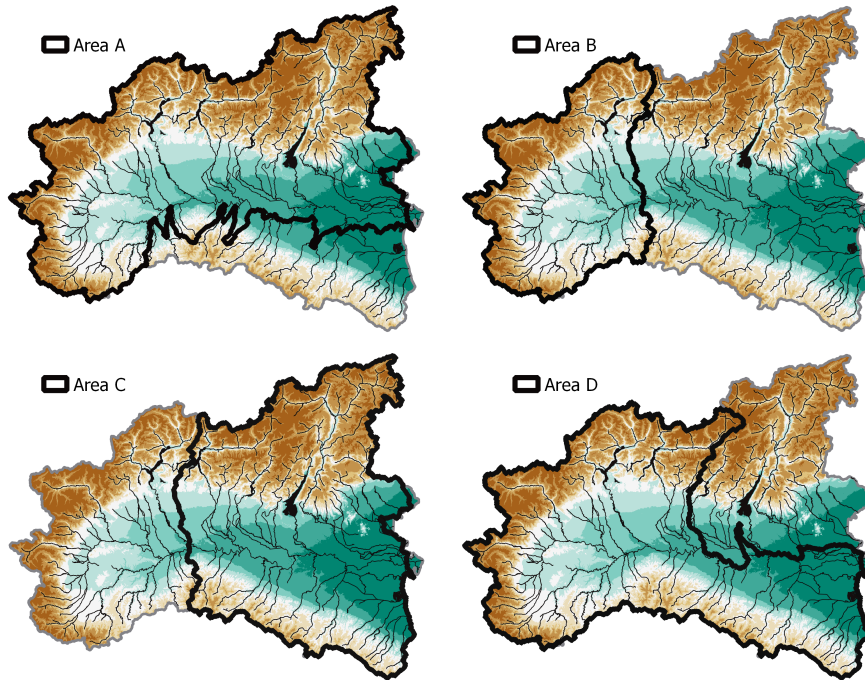
Figure 6. Training areas (bold contour) used for the geographical extrapolation experiments performed in phase (4), with major rivers and lakes higlighted in black

5.1 Delineation of flood-prone areas in interpolation mode

Figure 7 represents the flood susceptibility map obtained with the classifier DT model trained within the random 85% of the 2 km buffer calibration area (i.e. multivariate flood susceptibility map). To understand the quality of the proposed approach and profitably discuss the results, Figure 8 illustrates the map produced with the univariate benchmark approach set up in the same area. Relevant performance metrics for multivariate and univariate models are reported in rows 1 and 2 of Table 1, respectively. Figure 7 and Table 1 highlight that the DT flood susceptibility map is strongly consistent with the target map PGRA P1. Also, the model produces a rather detailed mapping across floodplains of minor streams (i.e. exhaustiveness, as defined in Sect. 3); in particular, it can be observed in Figure 7 that the zones where the target map has high exhaustiveness (e.g., northwestern portion of the study area) are mapped with slightly lower exhaustiveness by the DT model, while the DT output is more detailed in floodplain of minor streams than the target map, where the latter is lacking exhaustiveness (e.g., northeastern part).

Figure 7 shows that GFI uniformly and exhaustively estimates flood susceptibility along all minor streams in mountain areas, but tends to severely overestimate the size of flood-prone areas in predominantly flat regions.

The first line of Table 3 reports the Gini importance for the classifier DT: HAND scores about 65%, followed by elevation (16.5%) and GFI (10.5%).
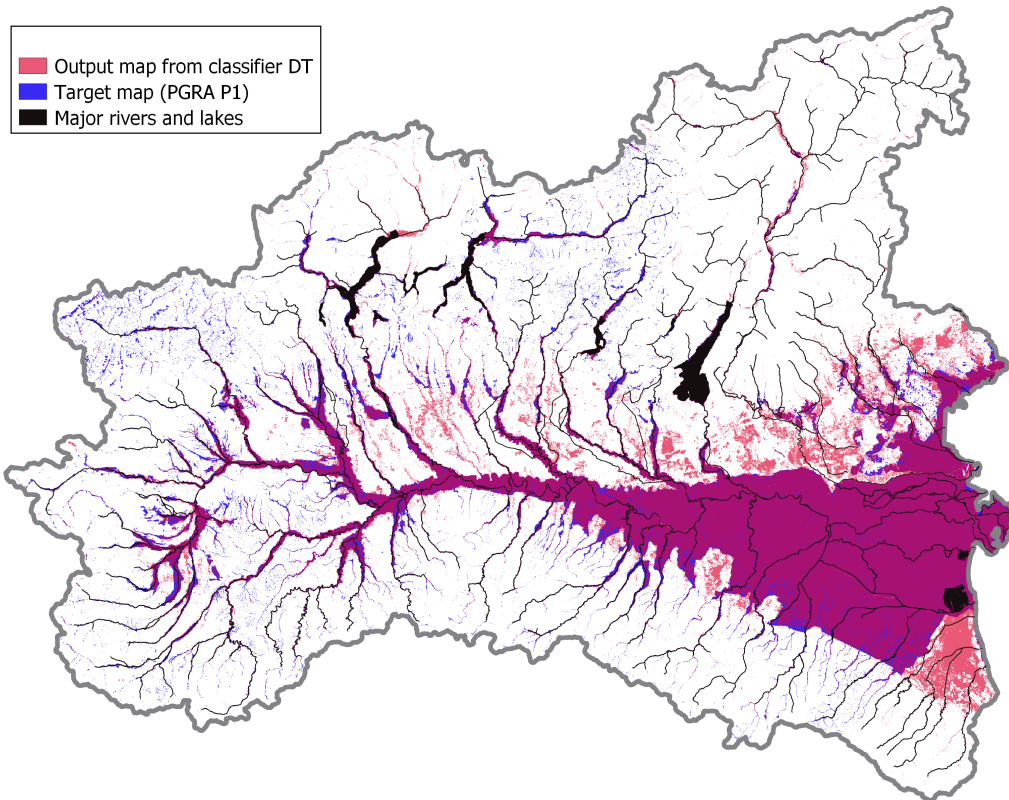
Figure 7. Multivariate 500-year flood susceptibility map for the study area (red); target flood hazard map (PGRA P1, blue); purple indicates overlaying areas

Table 1. Classification problem: performance metrics for the multivariate (classifier DTs) and univariate (classifier GFI) flood susceptibility maps; target flood hazard map for both approaches: PGRA P1. The reported values have been converted from the interval 0-1 to the percentage notation. The best testing metrics values are reported in bold, the worst ones in italic (the first line should be compared with the second one; the last four lines should be compared to each other)

Model	Training performance				Test performance			
	TSS	ACC	PPV	TPR	TSS	ACC	PPV	TPR
Classifier DT - interpolation	80%	93%	89%	84%	**78%**	**92%**	**88%**	*83%*
Classifier GFI - benchmark	69%	84%	66%	87%	*69%*	*84%*	*66%*	**87%**
Classifier DT trained in A	75%	92%	86%	78%	56%	83%	**88%**	61%
Classifier DT trained in B	61%	93%	82%	64%	**65%**	85%	80%	75%
Classifier DT trained in C	82%	92%	89%	88%	*33%*	**88%**	71%	*35%*
Classifier DT trained in D	80%	94%	91%	93%	63%	*79%*	*53%*	**87%**
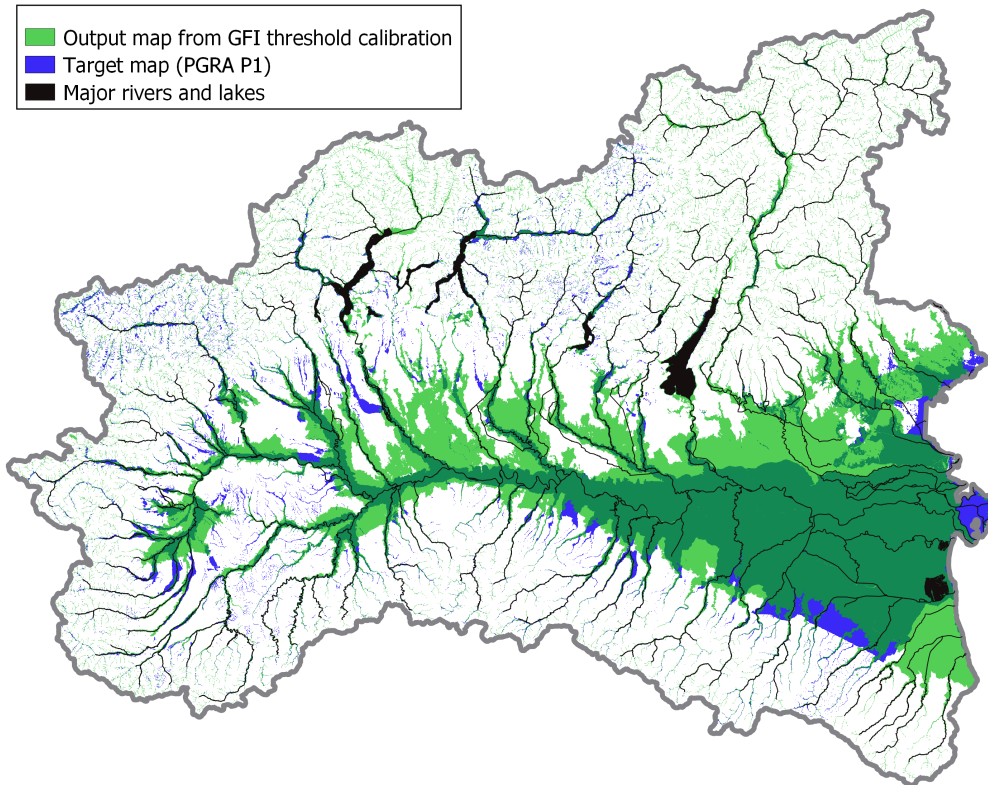
Figure 8. Binary flood susceptibility map resulting from a univariate analysis (morphometric index: GFI, light green); target flood hazard map (PGRA P1, blue); dark green indicates overlaying areas

5.2 Prediction of flood hazard intensity in interpolation mode

305 Figure 9 illustrates expected maximum inundation water depths as predicted through the regressor DT trained within the random 85% of the 5 km buffer calibration area; relevant performance metrics can be found in the first row of Table 2. Figure 9 and Table 2 show good performance of the DT model for the regression problem. It is worth noting here that the exhaustiveness of the DT water-depth map is considerably higher than that of the reference map (i.e. JRC 100). This result was expected due to the focus of JRC 100 on larger catchments.

310 The data density plot in Figure 10 depicts the relationship between target and predicted water depths for the test set focusing on true positives (i.e. both target and predicted water depths are higher than 0.0 m) and neglecting water depths higher than $3.5m$ (neglected pairs, beyond axes' limits, are 4.2% of the total).

The second row of Table 3 shows that the most informative GD is GFI (63.7%), followed by elevation (20.7%) and slope (5.4%).
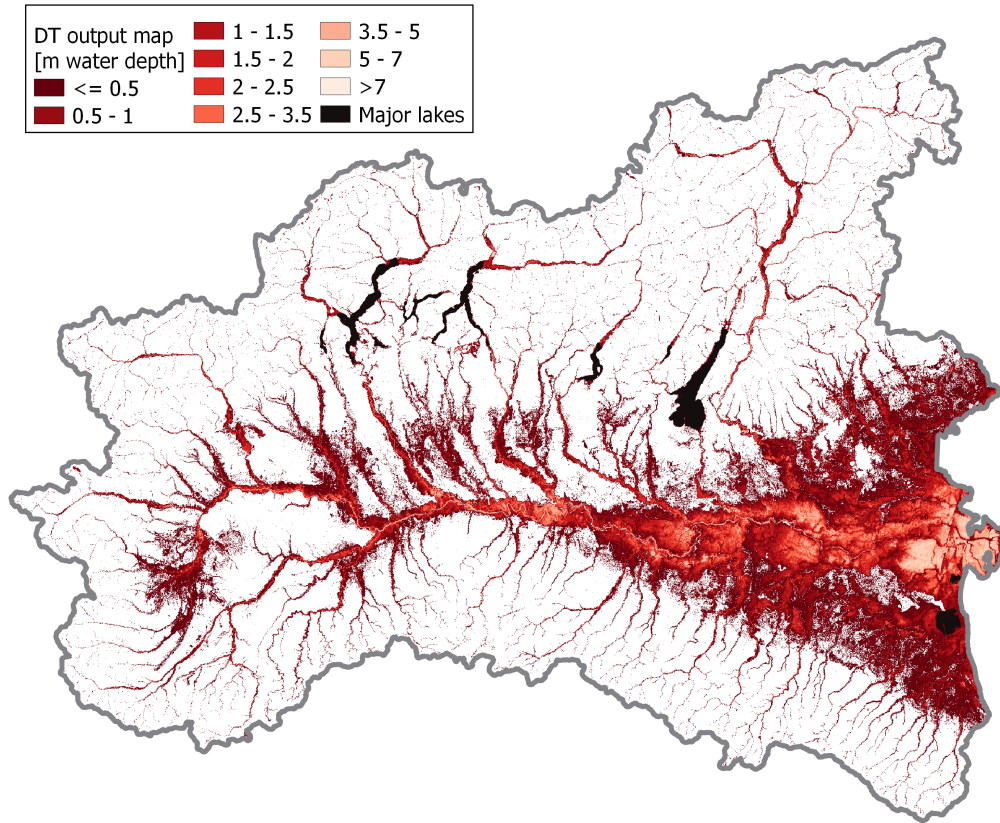
Figure 9. Multivariate water-depth hazard map obtained with regressor DT in interpolation mode (target flood hazard map: JRC 100)

Table 2. Regression problem: performance metrics for the multivariate water-depth output maps obtained with the regressor DTs (target flood hazard map: JRC 100); the best testing metrics values are reported in bold, the worst ones in italics

Model	Training performance			Test performance		
	R^2	MSE	MAE	R^2	MSE	MAE
Regressor DT - interpolation	0.726	0.227	0.393	**0.692**	**0.242**	**0.439**
Regressor DT trained in A	0.709	0.240	0.443	-0.029	1.100	0.547
Regressor DT trained in B	0.606	0.145	0.284	*-2.110*	*5.208*	*1.283*
Regressor DT trained in C	0.711	0.281	0.467	**0.333**	**0.623**	**0.264**
Regressor DT trained in D	0.741	0.251	0.380	0.175	1.109	0.417

315   5.3   Multivariate flood hazard modelling in extrapolation mode

Tables 1 (rows 3-6) and 2 (rows 2-5) report performance metrics for the geographical extrapolation experiments for the classification and regression problems, respectively, while Figures 11 and 12 depict the corresponding DT output maps.
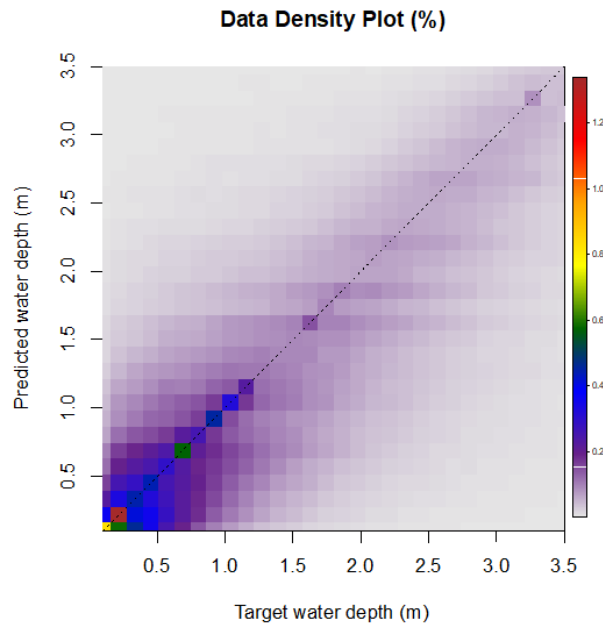
Figure 10. Data density plot (%) for target vs. predicted expected maximum water depth (target values: empirical JRC 100; predicted values: regressor DT applied to the test set)

With regards to the classification problem (Table 1), the performance metrics highlight a generalized good agreement with the target map. Figure 11 and section "Training performance" of Table 1 show that all models can accurately reproduce the target map in the training area, but they are quite inaccurate in the test area, as it is evident the difference between the two. In fact, concerning the test area, Table 1 shows that according to the true skill score (TSS), the best prediction in the test area is obtained using B as training area (TSS=65%), followed by D (TSS=63%) and A (TSS=56%), respectively. The same table section shows that the best results are obtained when training on area C if one focuses on accuracy (ACC=88%), followed by B (ACC=85%) and A (ACC=83%). According to precision (PPV), the best result is obtained training the model on area A (PPV=88%), while it is D according to recall (TPR=87%).

Concerning the regression problem, worse predictive skill in geographical extrapolation is observed in Table 2. Differently from the classification, performance metrics for the regression problem are in good agreement among each other, showing that area C has the better results, while area B is the worst. On the other hand, Figure 12 suggests that water depth estimation in the test area is quite reliable in all the cases, with the exception of the DT trained in area B.

Focusing on Gini importance, Table 3 clearly shows that regressor DTs (rows 7-10) are characterized by similar structures regardless of the training areas: GFI is always ranked first in terms of relevance, followed by elevation and slope. This is not true for the classification problem (rows 3-6): in this case, classifiers DTs identified four different training areas have different
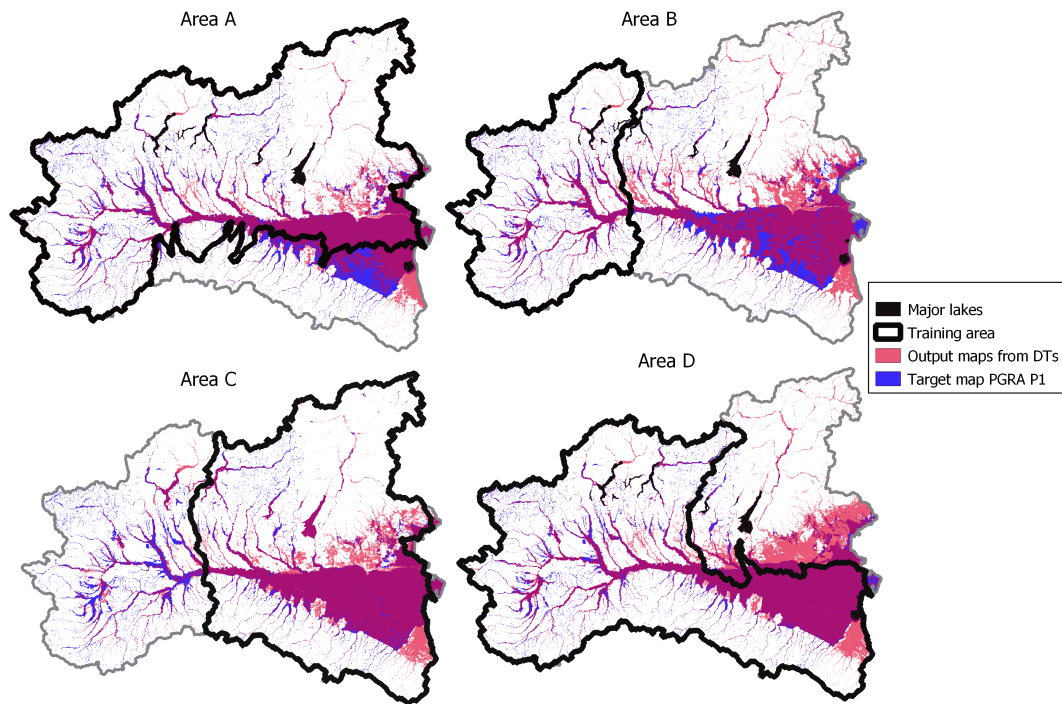
Figure 11. Geographical extrapolation for the classification problem: multivariate flood susceptibility maps obtained from classifier DTs (red); target flood hazard map (PGRA P1, blue); purple indicates overlaying areas

structures, in which the most informative geomorphic descriptor can be alternatively GFI, or HAND, or the elevation; this latter is always ranked second.

335 6 Discussion

6.1 Can we profit from a blend of various geomorphic descriptors for flood hazard assessment and mapping?

The first goal of the present research is the evaluation of the improvement which can be obtained by applying a machine-learning aided multivariate DEM-based flood hazard assessment relative to a univariate DEM-based approach. First, regarding the classification problem (i.e., differentiation between flood-prone and flood-free areas), the outcomes reported in Figures 7-8

340 and Table 1 (rows 1-2) suggest that the combination of multiple geomorphic descriptors (GDs) increases the comprehensiveness of the morphological description of the study area, and the resulting multivariate data-driven model can reproduce the reference flood hazard map in a significantly enhanced way relative to a univariate approach adopting a single GD. This is particularly visible from the lower extension of wrongly-predicted areas (i.e., false positive, or FP, and false negative, or FN) in the classifier DT output map (ligth red and blue areas in Figure 7) relative to the GFI output map (light green and blue areas
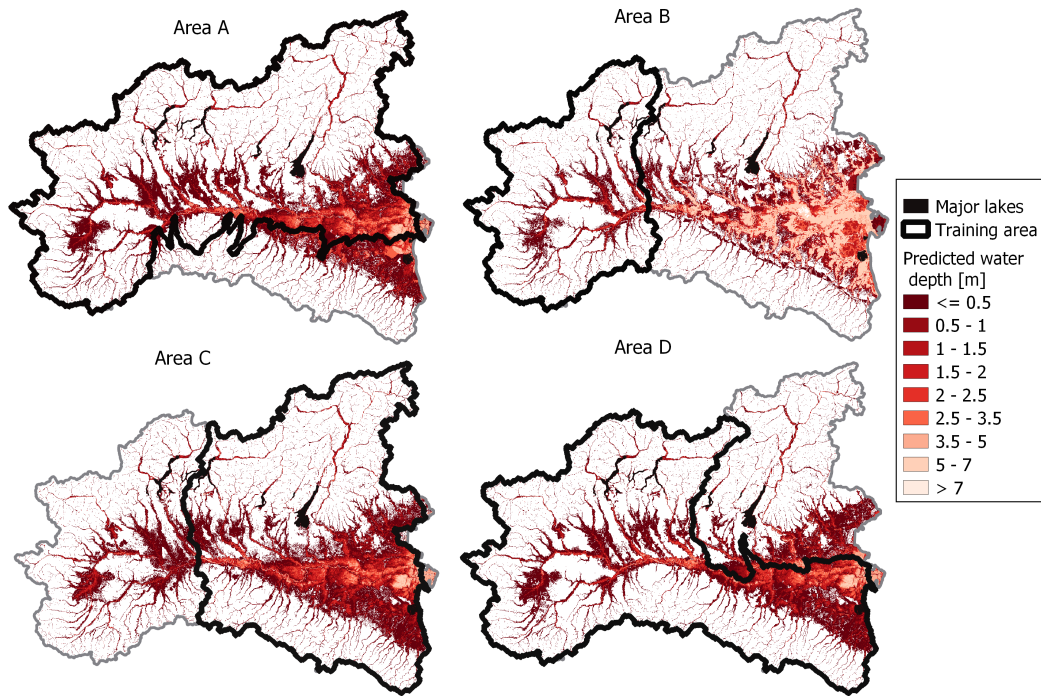
Figure 12. Geographical extrapolation for the regression problem: multivariate flood susceptibility maps obtained from regressor DTs (see also Figure 4, target flood hazard map: JRC 100)

Table 3. Gini importance of the selected input features computed for the DTs trained in phase (4); the highest value for each DT is highlighted in bold, the lowest in italic

Model	elevation	sd8	D	HAND	GFI	LGFI	TI_m
Classifier DT - interpolation	16.5%	3.5%	2.8%	**65.6%**	10.5%	0.6%	*0.4%*
Regressor DT - interpolation	20.7%	5.4%	2.0%	4.8%	**63.7%**	1.8%	*1.6%*
Classifier DT trained in A	10.2%	6.8%	2.2%	8.0%	**71.6%**	*0.3%*	0.8%
Classifier DT trained in B	9.8%	9.8%	3.8%	**60.0%**	11.8%	4.2%	*0.4%*
Classifier DT trained in C	**74.3%**	2.3%	1.7%	9.7%	11.1%	0.6%	*0.1%*
Classifier DT trained in D	18.5%	2.8%	1.4%	**69.5%**	7.1%	0.4%	*0.3%*
Regressor DT trained in A	14.3%	3.6%	1.8%	3.5%	**73.2%**	2.3%	*1.3%*
Regressor DT trained in B	18.9%	3.8%	2.6%	4.2%	**66.7%**	2.0%	*1.9%*
Regressor DT trained in C	17.8%	3.1%	1.9%	4.3%	**69.2%**	2.5%	*1.2%*
Regressor DT trained in D	14.3%	3.9%	1.3%	4.0%	**74.7%**	*0.9%*	0.9%

in Figure 8).

Second, concerning the regression problem (i.e., prediction of the flood intensity, such as the expected maximum water-depth associated with a given probability of occurrence) the regressor DT considered for interpolation shows high accuracy in reproducing the target map. Also, it is worth highlighting that regressor DTs provide a direct estimate of this variable, relative to the traditional univariate DEM-based approaches, which usually requires the prior delineation of flood extent to compute water depth, as the elevation difference between the flood-extent border and each pixel (see Manfreda and Samela, 2019). Figure 10 highlights that the correlation between the predicted and target water depths can be improved, yet it also clearly shows that predictions for the test set are unbiased. It is worth mentioning here that the diagram neglects the true negatives (i.e. target and predicted water depths are equal to $0.0m$; 49.78% of the cases), false positives (i.e. only predicted water depths are equal to $0.0m$; 22.37% of the cases) and false negatives (i.e. only target water depth are equal to $0.0m$; 0.08%). While the occurrence of the most concerning cases (false negatives) is very limited, predictions show significant margins for improvement as far as the false positives are concerned. Nevertheless, it should also be recalled here that the target map by its own very nature neglects smaller streams (contributing area has to be higher than $500km^2$), whereas the decision tree regressor looks at morphology only and provides water depth predictions also for smaller streams (i.e. higher exhaustiveness, see Figure 9).

One of the most interesting aspects is the relevance that each GD assumes in the regressor DTs (see Table 3). It can be observed that all models rely mainly on one single GD, with Gini importance always in excess of 60%, but still, the multivariate analysis leads to significantly better results relative to the univariate one. Also, it is important to highlight that:

– While regressor DTs tend to depend mainly on the GFI, classifier DTs depend on HAND

– While the input GDs have quite a similar Gini importance hierarchy in regressor DTs, classifiers DTs assume different hierarchical structures depending on the considered training area

– All models agree in giving low Gini importance to LGFI and TI_m, probably due to redundant information relative to GFI

– Elevation is very often ranked second, always associated with significant importance

Overall, this suggests that regressor DTs tend to operate by correcting a baseline estimate that mostly relies on the GFI value. On the other hand, classifier DTs obtain their results by following different rules depending on the training data, and often prefer using lower-levels features relative to more complex indicators such as the GFI. This sensitivity to the training area makes difficult to set a priori weights to the GDs when building up the models. It should be kept in mind, however, that different Gini importances do not necessarily imply radically different classification rules, due to the existing correlations between the input features. Ideally, dedicated feature selection and importance analysis algorithms should be used to obtain deeper insight on how the different models come to their conclusions; we plan to investigate this line as part of future work.

6.2 Can we use simple ML techniques for effectively blending multiple GDs?

The second research question of the present study is wheter it is possible to obtain a good estimation of flood hazard by combining multiple GDs with low-complexity machine learning models. Differently from several other contributes in the

literature, we do not focus on model complexity nor on the comparison of different models (Wang et al., 2015; Khosravi et al., 2018; Mosavi et al., 2018; Arabameri et al., 2019; Costache et al., 2020). Instead, we prefer to select one simple model type (i.e., decision trees, DTs) and focus on the combination of the five innovative elements listed in the Introduction; in this

380 way, we can analyse the influence on the multivariate DEM-based approach of the preliminary steps, consisting in data pre-processing (i.e., selection and manipulation of input features, target maps, training set and test set). This is highly important, because machine learning models do not reproduce the dynamics of the water, as such, their performance is strictly linked to the data used for the training, that need to be handled very carefully.

As it is highlighted in Sect. 6.1, the outcomes of the study (Figures 8-9, Tables 1-2) clearly show that DTs can effectively

385 reproduce the target information (Figures 3-4) with high accuracy for both classification and regression problem, even if the resolution of the MERIT DEM (Yamazaki et al., 2017), from which the input GDs have been retrieved, is not very high. Indeed, even if regressor DTs necessarily implicate discretization of the output variable, in the present study large datasets and appropriate tree depth allow us to obtain wide ranges of different water depth values. Moreover, it is worth mentioning that the trained DTs estimate flood hazard associated with different minor streams that are neglected in the target maps (see red areas

390 in Figure 7; compare Figure 9 with Figure 4): due to the absence of information in these areas, it is not possible to assess the goodness of the models output, but this tendency of completing target information could be a key aspect for future applications to data-scarce regions, and thus, it could be considered as a promising characteristic of the models.

Overall, it is possible to observe that DTs are effective tools to combine GDs and estimate flood hazard. This indicates that proper data handling has a strong influence on the accuracy of the final estimation, which is comparable to the choice of a

395 given machine learning technique. In particular, we want to underline two elements of the presented approach that have great importance on the predictive skill. First, the utilization of flood hazard maps as target results in a large number of pixels for the training and test set, and therefore a very broad spectrum of hydrological/morphological characteristics, which represent a much more informative dataset relative to isolated points used by other authors for training more complex models (Lee et al., 2017; Khosravi et al., 2018; Arabameri et al., 2019; Janizadeh et al., 2019). Second, a sensible identification of a calibration

400 area is very important for a successful training, as it allows to neglect irrelevant pixels. To this aim, a preliminary sensitivity analysis might be very useful for identifying the optimal buffering radius around the target map (see Sect. 4.1), even if different approaches are proposed in the literature (e.g., Degiorgis et al., 2012). Indeed, in the case of application of DEM-based methods in data-scarce areas, where local flood-hazard modelling datasets may not be available, global or continental flood hazard maps produced by the European Joint Research Centre (Dottori et al., 2016, 2021) can be used as a target, as done in this study.

405 **6.3 Are these techniques capable of providing a reliable assessment of flood hazard over large areas in extrapolation?**

The evaluation of prediction accuracy for geographical extrapolation (i.e., applying the models in geographical areas, or watersheds, that have not been considered for parameterization and training) is a key and characteristic aspect of our study. On the one hand, performing predictions with new input data is a major problem for machine learning models; on the other hand, reaching good predictive skills in extrapolation is needed for future practical applications to data-scarce environments. What is

410 more interesting about this part is to understand the link between training and test performances: if the relationship between in-

put and target values, learnt by the model during the training, is also valid for the extrapolation region, accurate test predictions are obtained, but this depends strongly on the choice of input and target datasets for the training, which can be very difficult. Before addressing this very issue, a careful discussion of the resulting metrics and maps is required, as their interpretation is not straightforward.

415 With reference to the classification problem, each metric suggests a different training area as the best case, and this highlights how difficult it is to choose a single metric for describing the goodness of a model for a binary classification. Figure 11 and TSS values in rows 4-5 of Table 2 could suggest that Area B (test TSS=65%) has better extrapolation performance than Area C (test TSS=33%). On the contrary, ACC is similar for the two cases, and higher for Area C (ACC=88%) than for Area B (ACC=85%), suggesting that TSS is a more informative metrics than ACC in representing the model performance. On the

420 other hand, precision and recall appear to be quite unbalanced metrics, as areas A and D lead to test prediction with considerable overextension of FN and FP values, respectively (see Figure 11). Differently, regression metrics agree in pointing at the DT trained in B as the best case (Table 3). However, the absolute values of R^2, that depicts low-accuracy test predictions, do not reflect other metrics (MSE and MAE) and the output maps (Figure 12).

As expected, the choice of the training area has great influence on prediction accuracy. This is particularly visible for the clas-

425 sification problem: in Figure 11, the difference between metrics for training and test is striking. Nevertheless, this difference becomes less clear for the regression problem (Figure 12). The same observations are confirmed by Table 3, where evidence is given of different structures for the classifiers DTs, while the regressor DTs are all very similar. More in detail, the obtained results show that the extent of the training area has less importance than the quality of the input data that it contains. Perfect examples of this remark are classifiers DTs trained in A and D: even if both A and D are very wide, prediction over the test area

430 is affected by considerable errors. This happens because A does not include any part of the Apennines, while D ignores a large flat area in the eastearn coast, meaning that any geographical system corresponds to a specific relationship between input GDs and flood susceptibility, and thus it cannot be fully represented by a model trained with very different datasets. The comparison between area B and C is also meaningful: while the training in B leads to good test predictions for the classification, it is the worst case for the regression (the opposite is valid for C). This is probably due to the fact that area B contains useful information

435 to delineate flood-prone areas, as it represents the upstream section of Po river, but cannot adequately train a regressor DT, as it lacks high target values (i.e., high inundation water depths). To sum up, GDs combination with DTs is capable to provide quite a reliable estimation of flood hazard (i.e., flood-prone areas and maximum water depth) in extrapolation mode, but a careful choice of the training area is needed, where target and input dataset is complete and representative for the test area.

7 Conclusions and further steps

440 Our study analyses and compares data-driven and resource-efficient methods for assessing and mapping riverine flood hazard across large geographical areas. It illustrates the potential and limitations of combining different geomorphic descriptors by means of decision trees for delineating flood prone areas and for predicting the expected maximum water depths for a given return period. We focus on a large study area in Northern Italy (size $\sim 10^5 km^2$) containing Western, Central and part

of the Eastern Italian Alps, part of the Northern Apennines and the floodplains of a complex river-system including the main rivers Po, Adige, Brenta, Bacchiglione and Reno. The morphology of the study area is described by the Multi-Error-Remover Improved-Terrain model (MERIT DEM; Yamazaki et al., 2017), with a 90-meter resolution, approximately. Decision trees are trained using as input features the geomorphic descriptors retrieved from the MERIT DEM, and as target maps two different datasets: one representing flood extent with a reference return period of 500 years, and one representing expected maximum water depth for a 100-year return period scenario.

Relative to previous studies focusing on morphometric floodplain delineation and flood-hazard mapping (see e.g., Dodov and Foufoula-Georgiou , 2006; Nardi et al., 2006; Manfreda et al., 2011, 2014, 2015; Samela et al., 2017; De Risi et al., 2018) and machine-learning aided multivariate flood hazard mapping (see e.g., Gnecco et al., 2017; Arabameri et al., 2019; Janizadeh et al., 2019; Costache et al., 2020), our study is the first one of its kind that simultaneously combines the following five elements: (a) only strictly DEM-based morphometric data and indices are used for predicting flood hazard; (b) morphological characterization of flood hazard associated with a given probability of occurrence is studied separately as a classification problem (i.e., generation of binary flood hazard maps) and as a regression problem (i.e., prediction of expected maximum inundation water depth); (c) machine learning models (i.e., decision trees) are trained using pre-exhisting flood hazard maps as target information; (d) univariate geomorphological assessment of flood hazard (i.e., one geomorphic descriptor used as predictor) is thoroughly compared with a multivariate assessment, in which several DEM-based geomorphic descriptors are blended together by means of decision trees; (e) potential and accuracy of DEM-based flood hazard prediction is assessed in geographical extrapolation by applying models trained on specific geographical areas to different areas having diverse morphologic and/or hydrological features.

In particular, we address three main science questions: (1) can we profit from a blend of geomorphic descriptors to perform flood hazard mapping with respect to a univariate DEM-based approach? (2) Are decision trees a valid tool for combining multiple geomorphic descriptors? (3) Is this approach capable to predict flood hazard over large areas in geographical extrapolation? With reference to the first and second questions, delineation of flood-prone areas (i.e. binary flood susceptibility mapping) is derived with two methods: a univariate approach, consisting in the calibration of a threshold value for a given DEM-based morphometric index (i.e., Geomorphic Flood Index, GFI; see e.g., Samela et al., 2017), and the proposed decision tree for multivariate DEM-based classification. Also, prediction of the maximum inundation water depth associated with a 100-year return period has been carried out. As done in other studies (Tavares da Costa et al., 2019), buffer areas around the target flood-prone areas are defined, in order to discard pixels far from the main river network: the models are trained and tested with different sets, consisting respectively in randomly-selected 85% and 15% of the pixels contained in the buffer. The results obtained for the classification problem show high performance metrics in validation (overall true skill statistic TSS$\sim$80%, overall accuracy ACC$\sim$92%) relative to the univariate approach (overall TSS=69%, overall ACC=83%). In particular, the combination of DEM-based descriptors leads to much more accurate results in flood-prone areas delineation over predominantly flat regions. Concerning the regression problem, good performances are confirmed in validation as well (i.e. overall determination coefficient $R^2 \sim$0.7, overall mean absolute error MAE$\sim$0.4 m). Also, with reference to the third question, we test the proposed approach in a second mode, which we termed geographical extrapolation. We delineate four different subregions of the study

area to train classifier and regressor decision trees by selecting four areas belonging to four different hydrologically-coherent geographical systems. When tested on the remainders of the study area, the four different models show different extrapolation performances depending on the morphological features (e.g. Apennines vs. Alps) and the broadness of the hydrological conditions included in the training subregions. In particular, concerning the classification problem, models trained in areas containing headwater catchments of the main rivers can extrapolate better over the downsteam portions of the basins than vice versa. Concerning the regression problem, the selection of the training area must rely not only on these morphological and hydrological features, but also on the availability of a sufficently wide range of values for the target variable (i.e., maximum water depth in our case) within this area, in order to adequately train the model. This means that training in headwater catchment areas performs very poorly for extrapolating maximum water depth across downstream floodplains.

In general, we observe that multivariate DEM-based analysis by means of decision trees is very effective in estimating flood hazard relative to univariate approach, and that these techniques have good potential in extrapolation mode as well. Moreover, output of multivariate DEM-based flood hazard assessment studies may represent a very useful complement to existing large scale flood hazard maps for two reasons: (1) they omogenize mapping when the existing maps have different levels of detail in different regions (e.g., in situations in which the large scale map consists of the merger of maps from different local authorities, which applied different flood hazard assessment criteria and methods); (2) they contribute to assessing the hazard level also in areas not inlcuded in the original mapping (e.g., when smaller river catchments have been neglected).

Different elements of this work can be further examined in future studies, in order to deepen the collective knowledge and understanding of the DEM-based multivariate techniques. First, classifier and regressor decision trees could be compared with other multivariate approaches, whose training is based on different target maps (e.g., inundation maps derived from satellite products). Second, finer resolution DEMs could be used, in order to increase the accuracy of the morphological description of the study area. Third, to further enhance the input information, soil and climate data (e.g., permeability and precipitation) could be added beside geomorphic descriptors. Finally, more complex machine learning models should be tested, for better characterizing the impact of selecting a given technique on the accuracy of flood hazard assessment.

Author contributions. A.M. designed and performed the experiments, wrote the codes and derived the models; M.L. had a key role in the application of machine learning techniques and the definition of the methodology. A.C. supervised and conceptualized the project. S.P. contributed in supervising the project and provided technical support. F.L.C. and A.T. took part in analysing and discussing the results. A.M. wrote the first version of the manuscript, and all the authors helped in writing the final one.

Competing interests. The authors declare that they have no conflict of interest.

Acknowledgements. The authors would like to thankfully acknowledge Leithà S.r.l. - Unipol Group (regional research grant: "Stima della pericolosità idraulica del territorio italiano") and Autorità di bacino distrettuale del fiume Po (regional research grant: "Idrologia di piena nel distretto del Po") for their financial support and access to data. The authors gratefully aknowledge the use of Free and Open Source Software, in particular Python (Van Rossum et al., 1995), Scikit-learn (Pedregosa et al., 2011), QGIS (QGIS Development Team, 2021), GRASS GIS (GRASS Development Team, 2019) and TauDEM (Tarboton, 2003).

References

Alfieri, L., Salamon, P., Bianchi, A., Neal, J., Bates, P., Feyen, L.: Advances in pan-European flood hazard mapping, Hydrol. Process. 28, 4067–4077, https://doi.org/10.1002/hyp.9947, 2018.

515 Alfieri, L., Salamon, P., Pappenberger, F., Wetterhall, F., Thielen, J.: Operational early warning systems for water-related hazards in Europe, Environ. Sci. Policy 21, 35–49, https://doi.org/10.1016/j.envsci.2012.01.008, 2012.

Arabameri, A., Rezaei, K., Cerdá, A., Conoscenti, C., Kalantari, Z.: A comparison of statistical methods and multi-criteria decision making to map flood hazard susceptibility in Northern Iran, Sci. Total Environ. 660, 443–458, https://doi.org/10.1016/j.scitotenv.2019.01.021, 2019.

520 Bartholmes, J.C., Thielen, J., Ramos, M.H., Gentilini, S.: The european flood alert system EFAS – Part 2: Statistical skill assessment of probabilistic and deterministic operational forecasts, Hydrol. Earth Syst. Sci. 13, 141–153, https://doi.org/10.5194/hess-13-141-2009, 2009.

Bellos, V., Tsakiris, G.: A hybrid method for flood simulation in small catchments combining hydrodynamic and hydrological techniques, J. Hydrol. 540, 331–339, https://doi.org/10.1016/j.jhydrol.2016.06.040, 2016.

525 Breiman, L., Friedman, J., Stone, C. J., Olshen, R.A.: Classification and regression trees, Repr. ed. Chapman & Hall [u.a.], Boca Raton, 1998.

Brunetti, M., Maugeri, M., Nanni, T., Navarra, A.: Droughts and extreme events in regional daily Italian precipitation series, Int. J. Climatol. 22, 543–558, https://doi.org/10.1002/joc.751, 2002.

Costabile, P., Costanzo, C., Macchione, F.: Comparative analysis of overland flow models using finite volume schemes, J. Hydroinformatics 14, 122–135, https://doi.org/10.2166/hydro.2011.077, 2012.

530 Costache, R., Pham, Q.B., Avand, M., Thuy Linh, N.T., Vojtek, M., Vojteková, J., Lee, S., Khoi, D.N., Thao Nhi, P.T., Dung, T.D.: Novel hybrid models between bivariate statistics, artificial neural networks and boosting algorithms for flood susceptibility assessment, J. Environ. Manage. 265, 110485, https://doi.org/ 10.1016/j.jenvman.2020.110485, 2020.

De Risi, R., Jalayer, F., De Paola, F., Lindley, S.: Delineation of flooding risk hotspots based on digital elevation model, calculated and historical flooding extents: the case of Ouagadougou, Stoch. Environ. Res. Risk Assess. 32, 1545–1559, https://doi.org/10.1007/s00477-
535 017-1450-8, 2018.

Degiorgis, M., Gnecco, G., Gorni, S., Roth, G., Sanguineti, M., Taramasso, A.C.: Classifiers for the detection of flood-prone areas using remote sensed elevation data, J. Hydrol. 470–471, 302–315, https://doi.org/10.1016/j.jhydrol.2012.09.006, 2012.

Di Baldassarre, G., Kooy, M., Kemerink, J.S., Brandimarte, L.: Towards understanding the dynamic behaviour of floodplains as human-water systems, Hydrol. Earth Syst. Sci. 17, 3235–3244, https://doi.org/10.5194/hess-17-3235-2013, 2013.

540 Dodov, B.A., Foufoula-Georgiou, E.: Floodplain Morphometry Extraction From a High-Resolution Digital Elevation Model: A Simple Algorithm for Regional Analysis Studies, IEEE Geosci. Remote Sens. Lett. 3, 410–413, https://doi.org/10.1109/LGRS.2006.874161, 2006.

Domeneghetti, A., Carisi, F., Castellarin, A., Brath, A.: Evolution of flood risk over large areas: Quantitative assessment for the Po river, J. Hydrol. 527, 809–823, https://doi.org/10.1016/j.jhydrol.2015.05.043, 2015.

545 Dottori, F., Salamon, P., Bianchi, A., Alfieri, L., Hirpa, F.A., Feyen, L.: Development and evaluation of a framework for global flood hazard mapping, Adv. Water Resour. 94, 87–102, https://doi.org/10.1016/j.advwatres.2016.05.002, 2016.

Dottori, F., Alfieri, L., Bianchi, A., Skoien, J., and Salamon, P.: A new dataset of river flood hazard maps for Europe and the Mediterranean Basin region, Earth Syst. Sci. Data Discuss. [preprint], https://doi.org/10.5194/essd-2020-313, in review, 2021.

Everitt, B.: The Cambridge dictionary of statistics, 2nd ed, Cambridge University Press, Cambridge, United Kingdom, 2002.

550   Faridani, F., Bakhtiari, S., Faridhosseini, A., Gibson, M.J., Farmani, R., Lasaponara, R.: Estimating Flood Characteristics Using Geomorphologic Flood Index with Regards to Rainfall Intensity-Duration-Frequency-Area Curves and CADDIES-2D Model in Three Iranian Basins, Sustainability 12, 7371, https://doi.org/10.3390/su12187371, 2020.

Gnecco, G., Morisi, R., Roth, G., Sanguineti, M., Taramasso, A.C.: Supervised and semi-supervised classifiers for the detection of flood-prone areas, Soft Comput. 21, 3673–3685, https://doi.org/10.1007/s00500-015-1983-z, 2017.

555   GRASS Development Team: Geographic Resources Analysis Support System (GRASS) Software, Version 7.6, Open Source Geospatial Foundation, https://grass.osgeo.org, 2019.

Guha-Sapir, D., Hoyois, Ph., Wallemacq P. Below. R.: Annual Disaster Statistical Review 2016: The Numbers and Trends, CRED, Brussels, Belgium, 2016.

Hastie, T., Tibshirani, R., Friedman, J.: The Elements of Statistical Learning, Springer Series in Statistics, Springer New York, New York,
560   NY, https://doi.org/10.1007/978-0-387-84858-7, 2009.

Ho, W., Xu, X., Dey, P.K.: Multi-criteria decision making approaches for supplier evaluation and selection: A literature review, Eur. J. Oper. Res. 202, 16–24, https://doi.org/10.1016/j.ejor.2009.05.009, 2010.

Horritt, M.S., Bates, P.D.: Evaluation of 1D and 2D numerical models for predicting river flood inundation, J. Hydrol. 268, 87–99, https://doi.org/10.1016/S0022-1694(02)00121-X, 2002.

565   Hosseiny, H., Nazari, F., Smith, V., Nataraj, C.: A Framework for Modeling Flood Depth Using a Hybrid of Hydraulics and Machine Learning, Sci. Rep. 10, 8222, https://doi.org/10.1038/s41598-020-65232-5, 2020.

ISPRA: Landslides and Floods in Italy: Hazard and Risk Indicators – Summary Report 2018, ISPRA Reports 287/bis/2018, ISBN: 978-88-448-0934-0938, 2018.

Janizadeh, S., Avand, M., Jaafari, A., Phong, T.V., Bayat, M., Ahmadisharaf, E., Prakash, I., Pham, B.T., Lee, S.: Prediction Suc-
570   cess of Machine Learning Methods for Flash Flood Susceptibility Mapping in the Tafresh Watershed, Iran, Sustainability 11, 5426, https://doi.org/10.3390/su11195426, 2019.

Jongman, B., Koks, E.E., Husby, T.G., Ward, P.J.: Increasing flood exposure in the Netherlands: implications for risk financing, Nat. Hazards Earth Syst. Sci. 14, 1245–1255, https://doi.org/10.5194/nhess-14-1245-2014, 2014.

Kirkby, MJ: Hydrograph modelling strategies, in: Processes in physical and human geography, Heinemann, Oxford, pp 69–90, 1975.

575   Khosravi, K., Pham, B.T., Chapi, K., Shirzadi, A., Shahabi, H., Revhaug, I., Prakash, I., Tien Bui, D.: A comparative assessment of decision trees algorithms for flash flood susceptibility modeling at Haraz watershed, northern Iran, Sci. Total Environ. 627, 744–755, https://doi.org/10.1016/j.scitotenv.2018.01.266, 2018.

Lee, Sunmin, Kim, J.-C., Jung, H.-S., Lee, M.J., Lee, Saro: Spatial prediction of flood susceptibility using random-forest and boosted-tree models in Seoul metropolitan city, Korea, Geomat. Nat. Hazards Risk 8, 1185–1203, https://doi.org/10.1080/19475705.2017.1308971,
580   2017.

Manfreda, S., Sole, A., Fiorentino, M.: Can the basin morphology alone provide an insight into floodplain delineation?, in: Flood Recovery, Innovation and Response I, edited by: Proverbs, D., Brebbia, C.A. and Penning-Roswell, E., WITpress, London, England, pagg. 47–56, https://doi.org/10.2495/FRIAR080051, 2008.

Manfreda, S., Di Leo, M., Sole, A.: Detection of Flood-Prone Areas Using Digital Elevation Models, J. Hydrol. Eng. 16, 781–790,
585   https://doi.org/10.1061/(ASCE)HE.1943-5584.0000367, 2011.

Manfreda, S., Nardi, F., Samela, C., Grimaldi, S., Taramasso, A.C., Roth, G., Sole, A.: Investigation on the use of geomorphic approaches for the delineation of flood prone areas, J. Hydrol. 517, 863–876, https://doi.org/10.1016/j.jhydrol.2014.06.009, 2014.

Manfreda, S., Samela, C., Gioia, A., Consoli, G.G., Iacobellis, V., Giuzio, L., Cantisani, A., Sole, A.: Flood-prone areas assessment using linear binary classifiers based on flood maps obtained from 1D and 2D hydraulic models, Nat. Hazards 79, 735–754, https://doi.org/10.1007/s11069-015-1869-5, 2015.

Manfreda, S., Samela, C.: A digital elevation model based method for a rapid estimation of flood inundation depth, J. Flood Risk Manag. 12, https://doi.org/10.1111/jfr3.12541, 2019.

Mosavi, A., Ozturk, P., Chau, K.: Flood Prediction Using Machine Learning Models: Literature Review, Water 10, 1536, https://doi.org/10.3390/w10111536, 2018.

Nardi, F., Vivoni, E.R., Grimaldi, S.: Investigating a floodplain scaling relation using a hydrogeomorphic delineation method: HYDROGEOMORPHIC FLOODPLAIN DELINEATION METHOD, Water Resour. Res. 42, https://doi.org/10.1029/2005WR004155, 2006.

Noman, N.S., Nelson, E.J., Zundel, A.K.: Review of Automated Floodplain Delineation from Digital Terrain Models, J. Water Resour. Plan. Manag. 127, 394–402, https://doi.org/10.1061/(ASCE)0733-9496(2001)127:6(394), 2001.

OpenStreetMap contributors: Planet dump retrieved from https://planet.osm.org, https://www.openstreetmap.org, 2017.

Pedregosa, F., Varoquaux, G., Gramfort, A., Michel, V., Thirion, B., Grisel, O., Blondel, M., Müller, A., Nothman, J., Louppe, G., Prettenhofer, P., Weiss, R., Dubourg, V., Vanderplas, J., Passos, A., Cournapeau, D., Brucher, M., Perrot, M., Duchesnay, É.: Scikit-learn: Machine Learning in Python, J. Mach. Learn. Res. 12, ArXiv12010490 C, 2011.

Persiano, S., Ferri, E., Antolini, G., Domeneghetti, A., Pavan, V., Castellarin, A.: Changes in seasonality and magnitude of sub-daily rainfall extremes in Emilia-Romagna (Italy) and potential influence on regional rainfall frequency estimation, J. Hydrol. Reg. Stud. 32, 100751, https://doi.org/10.1016/j.ejrh.2020.100751, 2020.

QGIS Development Team: QGIS Geographic Information System, QGIS Association, https://www.qgis.org, 2021.

Rennó, C.D., Nobre, A.D., Cuartas, L.A., Soares, J.V., Hodnett, M.G., Tomasella, J., Waterloo, M.J.: HAND, a new terrain descriptor using SRTM-DEM: Mapping terra-firme rainforest environments in Amazonia, Remote Sens. Environ. 112, 3469–3481, https://doi.org/10.1016/j.rse.2008.03.018, 2008.

Requena, A.I., Prosdocimi, I., Kjeldsen, T.R., Mediero, L.: A bivariate trend analysis to investigate the effect of increasing urbanisation on flood characteristics, Hydrol. Res. 48, 802–821, https://doi.org/10.2166/nh.2016.105, 2017.

Samela, C., Troy, T.J., Manfreda, S.: Geomorphic classifiers for flood-prone areas delineation for data-scarce environments, Adv. Water Resour. 102, 13–28, https://doi.org/10.1016/j.advwatres.2017.01.007, 2017.

Samela, C., Albano, R., Sole, A., Manfreda, S.: A GIS tool for cost-effective delineation of flood-prone areas, Comput. Environ. Urban Syst. 70, 43–52, https://doi.org/10.1016/j.compenvurbsys.2018.01.013, 2018.

Tarboton, D.G., Bras, R.L., Rodriguez-Iturbe, I.: On the extraction of channel networks from digital elevation data, Hydrol. Process. 5, 81–100, https://doi.org/10.1002/hyp.3360050107, 1991.

Tarboton, D. G.: Terrain Analysis Using Digital Elevation Models in Hydrology, 23rd ESRI International Users Conference, San Diego, California, 2003.

Tavares da Costa, R., Manfreda, S., Luzzi, V., Samela, C., Mazzoli, P., Castellarin, A., Bagli, S.: A web application for hydrogeomorphic flood hazard mapping, Environ. Model. Softw. 118, 172–186, https://doi.org/10.1016/j.envsoft.2019.04.010, 2019.

Tavares da Costa, R., Zanardo, S., Bagli, S., Hilberts, A.G.J., Manfreda, S., Samela, C., Castellarin, A.: Predictive Modeling of Envelope Flood Extents Using Geomorphic and Climatic-Hydrologic Catchment Characteristics, Water Resour. Res. 56, https://doi.org/10.1029/2019WR026453, 2020.

625 Triantaphyllou, E.: Multi-Criteria Decision Making Methods, in: Multi-Criteria Decision Making Methods: A Comparative Study, Applied Optimization, Springer US, Boston, MA, pp. 5–21. https://doi.org/10.1007/978-1-4757-3157-6, 2000.

Uboldi, F., Lussana, C.: Evidence of non-stationarity in a local climatology of rainfall extremes in northern Italy: NON-STATIONARITY IN A LOCAL CLIMATOLOGY OF RAINFALL EXTREMES, Int. J. Climatol. 38, 506–516, https://doi.org/10.1002/joc.5183, 2018.

Van Rossum, G., Drake Jr, F.L.: Python reference manual, Centrum voor Wiskunde en Informatica Amsterdam, 1995.

630 Wang, Z., Lai, C., Chen, X., Yang, B., Zhao, S., Bai, X.: Flood hazard risk assessment model based on random forest, J. Hydrol, 527, 1130–1141. https://doi.org/10.1016/j.jhydrol.2015.06.008, 2015.

Williams, W.A., Jensen, M.E., Winne, J.C., Redmond, R.L.: An Automated Technique for Delineating and Characterizing Valley-Bottom Settings, in: Monitoring Ecological Condition in the Western United States, edited by: Sandhu, S.S., Melzian, B.D., Long, E.R., Whitford, W.G., Walton, B.T., Springer Netherlands, Dordrecht, pp. 105–114, https://doi.org/10.1007/978-94-011-4343-1_10, 2000.

635 Yamazaki, D., Ikeshima, D., Tawatari, R., Yamaguchi, T., O'Loughlin, F., Neal, J.C., Sampson, C.C., Kanae, S., Bates, P.D.: A high-accuracy map of global terrain elevations: Accurate Global Terrain Elevation map, Geophys. Res. Lett. 44, 5844–5853, https://doi.org/10.1002/2017GL072874, 2017.

Youden, W.J.: Index for rating diagnostic tests, Cancer 3, 32–35, https://doi.org/10.1002/1097-0142(1950)3:1<32::aid-cncr2820030106>3.0.co;2-3, 1950.